NANO LETTERS

2009
Vol. 9, No. 12
4158-4167

Stretched Extracellular Matrix Proteins Turn Fouling and Are Functionally Rescued by the Chaperones Albumin and Casein

William C. Little,[+] Ruth Schwartlander,[+] Michael L. Smith,[#] Delphine Gourdon, and Viola Vogel*

Department of Materials, ETH Zurich, CH-8093 Zurich, Switzerland

Received July 23, 2009

ABSTRACT

While evidence is mounting that cells exploit protein unfolding for mechanochemical signal conversion (mechanotransduction), what mechanisms are in place to deal with the unwanted consequences of exposing hydrophobic residues upon force-induced protein unfolding? Here, we show that mechanical chaperones exist that can transiently bind to hydrophobic residues that are freshly exposed by mechanical force. The stretch-upregulated binding of albumin or casein to fibronectin fibers is reversible and does not inhibit fiber contraction once the tension is released.

A decade after the birth of single-molecule mechanics,[1−3] it is well established that mechanical forces can unfold proteins, and the unfolding trajectories of many proteins have been experimentally mapped or simulated (as reviewed in refs 4−7). Proteins can refold reversibly once the force is sufficiently reduced.[8] Protein unfolding is physiologically significant, and cell-generated tensile forces can unfold extracellular[9−11] as well as intracellular[12,13] proteins. On the extracellular side, cell-generated forces are sufficient to stretch and then unfold fibronectin (Fn) fibers.[9−11] Some experimental evidence[14] and many predictions[15,16] have shown that forced unfolding may alter binding sites or expose otherwise cryptic molecular recognition sites of extracellular matrix (ECM) proteins. On the intracellular side, force-induced unfolding of p130cas can expose phosphorylation sites.[13] Mechanical stress applied by living cells to their surroundings ranges from 1 up to 10 nN per μm^2.[17−20]

While it is increasingly recognized that force-induced protein unfolding is an important motif by which cells can sense and respond to mechanical forces (mechanotransduction processes), protein unfolding may also have deleterious consequences. As for chemically or thermally denatured proteins, the mechanical exposure of hydrophobic residues should also lead to nonspecific protein adsorption, aggregation, and other processes that might be unwanted in a cellular environment. Mechanically stretched and unfolded proteins as well as protein fibers should thus turn fouling. Significantly though, the necessity of chaperones that transiently rescue the functions of mechanically unfolded proteins by inhibiting uncontrolled nonspecific binding has never been discussed before.

In order to block nonspecific protein binding and to prevent loss of protein function when in contact with hydrophobic surfaces, many molecules were developed by the biomaterials community to render surfaces nonfouling.[21] Biological analogues that can turn surfaces nonfouling are albumin and casein, which found widespread technical applications. Albumin, which comprises ∼55% of proteins in serum, is highly concentrated in the extracellular environment.[22−24] Its three homologous domains consist of two helical subdomains that in total provide a variety of binding sites for both hydrophobic and negatively charged hydrophilic moieties. Casein, comprising ∼75% of the protein found in mammalian milk, has a highly flexible amino acid chain with a large number of hydrophobic residues exposed due to its abundant proline residues.[25] To date, however, nothing is known about the binding behavior of albumin and casein to proteins that are mechanically stretched and unfolded. Albumin and casein have both been characterized as extracellular chaperones, after it was shown that they could antagonize aggregation of heat-denatured proteins and assist in their functional recovery,[22,24,26,27]

The objective of this study was to ask, first of all, whether the stretching of Fn fibers turns them fouling and, subse-

* To whom correspondence should be addressed. Address: Laboratory of Biologically Oriented Materials, Department of Materials, Wolfgang-Pauli-Strasse 10, HCI F 443, ETH Zurich, CH-8093 Zurich, Switzerland. Phone: +41 44 632 0887. Fax: +41 44 632 10 73. E-mail: viola.vogel@mat.ethz.ch.

[#] Current address: Boston University, Department of Biomedical Engineering, Boston, MA 02215.

[+] Authors contributed equally.

10.1021/nl902365z CCC: $40.75
Published on Web 09/10/2009

quently, whether the binding of albumin and casein to this ECM proteins is upregulated when stretched. To conduct quantitative assays with sufficient sensitivity, we chose to study fibers made from the ECM protein fibronectin (Fn) as a model system. Probing stretch-activated protein binding was made possible with a recently developed stretch assay that allows us to stabilize mechanically strained proteins in nonequilibrium structures and to read out their conformation optically with fluorescence resonance energy transfer (FRET).[9,10] To probe the adsorption and desorption kinetics as a function of the mechanical strain of fibrillar Fn, casein and albumin (labeled with a third fluorophore) were allowed to adsorb from solution. We further asked whether fibrillar Fn could refold once albumin was bound to stretched fibers and whether albumin would desorb once the force pulling on the fibers was released. Finally, we probed whether bound albumin blocks access to specific binding sites, with a focus on probing the cryptic binding sites that regulate Fn−Fn fibrillogenesis.

FRET-Based Stretch Assay to Mechanically Tune the Conformation of Fibrillar Fibronectin. To tune the conformation of Fn fibers in a controllable manner, Fn fibers were drawn manually from a concentrated Fn solution and deposited onto stretchable silicone sheets which were mounted onto a custom-built, uniaxial strain device.[14] The fibers parallel to the strain axis were stretched, whereas the vertically deposited fibers were relaxed. Absolute fiber strains were defined as $100(L\text{-}Lo)/Lo$ where L is the extended fiber length and Lo is the fiber length when fully relaxed (Klotzsch et al., submitted). To optically monitor conformational changes, in this large multimeric protein a small fraction of the plasma Fn was labeled with multiple donor and acceptor fluorophores.[9−11] Images were acquired, and the degree of FRET was measured, pixel-by-pixel, normalized by dividing the intensity of the acceptor channel by the intensity of the donor channel, hereafter referred to as I_A/I_D and visualized in false colors. Figure 1a shows that the stretching of Fn fibers alters their conformation, and thus false color, where the relaxed Fn fibers are red and the highly stretched fibers are bluish-green. The histogram of the corresponding I_A/I_D ratios is shown in Figure 1b, indicating two major conformational populations representing the stretched and relaxed fibers, respectively. Closer examination of each fiber indicates small pixel-to-pixel variations of Fn conformations. To calibrate the I_A/I_D ratios for every Fn batch, FRET-labeled Fn was also denatured in solution, where the onset of loss of secondary structure occurs at 1 M guanidine hydrochloride (GndHCl).[9−11,14,28−29] We have shown previously that this I_A/I_D ratio equals the ratio seen for Fn fibers strained 2−3 times their resting length[10,14] and that the stretching of freely suspended fibers beyond this mechanical strain causes a major increase in the exposure of cryptic sites buried in FnIII modules (Klotzsch et al., submitted).

Stretching of Fn Fibers Enhances the Nonspecific Binding of Albumin and Casein. To test whether albumin and casein display up-regulated adhesion to Fn fibers as a function of fiber extension, they were labeled with Alexa Fluor 633, a third, longer wavelength emitting fluorophore. When stretched or relaxed Fn fibers were exposed to a 0.1 g/L solution of either labeled bovine serum albumin (BSA) or labeled casein, images of fluorescent BSA or casein in Figure 1 show that a higher quantity of albumin (Figure 1a,c) and casein (Figure 1e,g) were bound to stretched (horizontal orientations) rather than to relaxed (vertical orientations) Fn fibers (see also Figure S4, Supporting Information). The pixel intensities of BSA and casein appear brighter on stretched fibers (Figure 1a). Since the number of Fn molecules per pixel volume changes as the fibers get stretched, we normalized the intensity of the soluble protein (i.e., BSA or casein) by the intensity of the fluorescently labeled fibrillar Fn in each pixel. Pixel-by-pixel, the intensity of Alexa 633-labeled soluble protein ($I_{Alexa633}$) was divided by the sum of Fn's donor and acceptor intensities ($I_D + I_A$) using the acquired FRET image with 488 nm excitation light. Similar results for normalized BSA and Fn binding were found when we simply used the intensity of the acceptor fluorophore with direct acceptor excitation at 543 nm (see Figure S3, Supporting Information). Figure 1d,h shows the ratio of the Alexa 633 intensity of bound BSA and casein (Figure 1c,h, respectively) to the sum of $I_A + I_D$ for all fiber pixels in the fields of view shown in Figure 1a,e. The data are shown as contour plots where the density of ratios is mapped to an artificial color code.

The binding of both BSA and casein increases as Fn is progressively stretched. The transition from low binding to increased binding occurs when relaxed fibers (0% strain) are stretched to about 100−140% strain. When the Fn fibers are stretched further, albumin and casein binding levels plateau. It was not possible to determine which soluble protein had the maximum amount of binding at a given strain state since the ratio of Alexa 633 to Fn-DA $I_A + I_D$ depends upon the labeling ratio of BSA and casein. However, the relative increase in binding was even more pronounced with casein (Figure 1h).

While this first set of experiments was conducted under physiological buffer conditions, the experiment was repeated in the presence of 10% fetal calf serum. We labeled all proteins in whole bovine serum with Alexa Fluor 633 and repeated the colocalization binding experiments described above (Figure S4, Supporting Information). Again, we observed an increased albumin binding as the fibers were stretched, demonstrating that the increased binding behavior to mechanically stretched Fn fibers is physiologically relevant. While the results were similar to albumin and casein in that a significant increase in serum binding was observed up to a 100−140% absolute strain (Figure S4, Supporting Information), beyond this point, no significant increase in binding was detected.

As a negative control of a binding site that is exposed under equilibrium, we also investigated how the L8 monoclonal antibody, which binds only within residues 526−675 spanning FnI_9 and $FnIII_1$,[30] adheres to stretched versus relaxed Fn following the same colocalization procedure. Contrary to the results from all other proteins examined in this report, the L8 antibody showed decreased binding to stretched Fn fibers (Figure 1i-j). L8 binding to Fn fibers

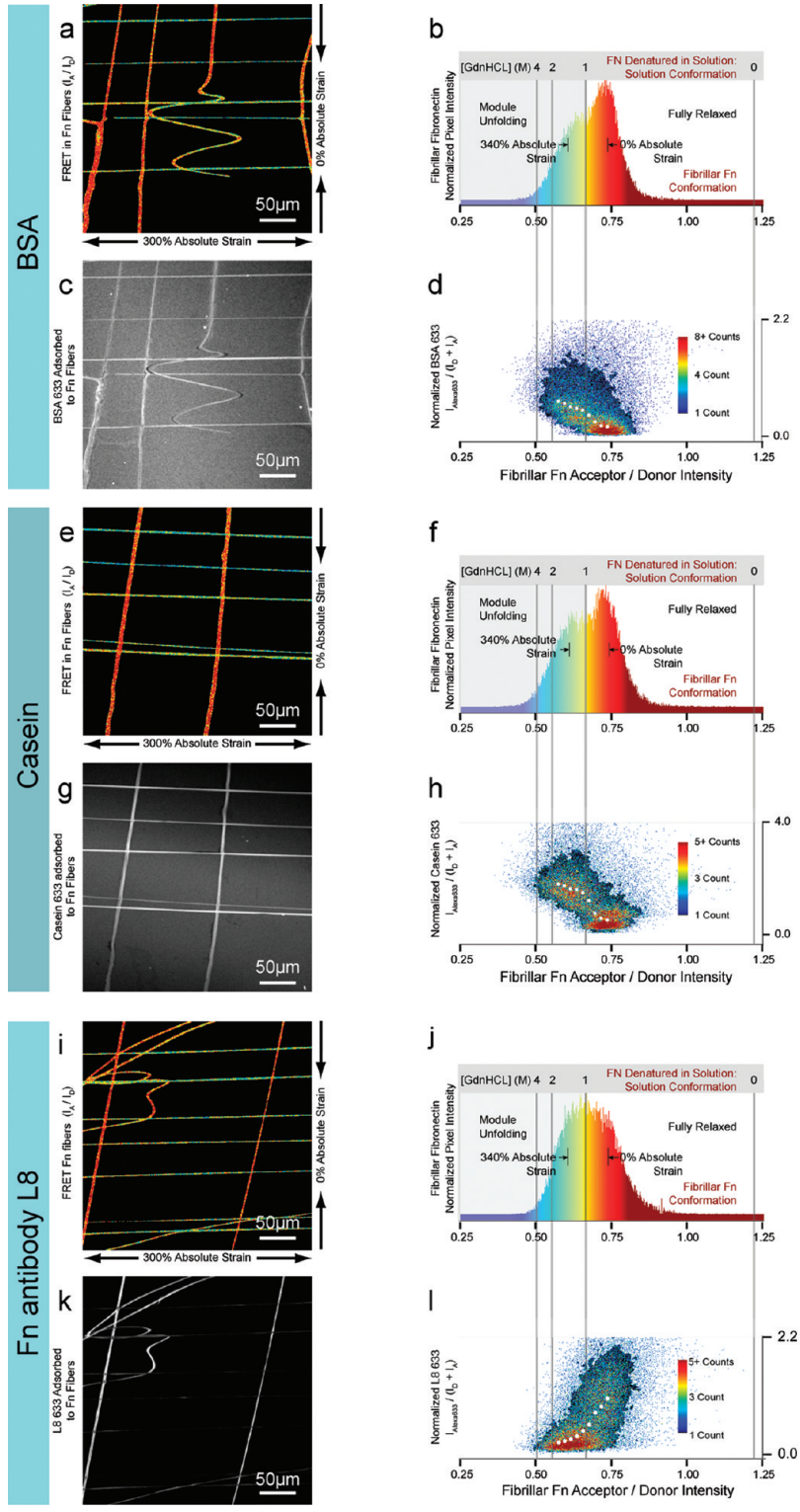

Figure 1. Colocalization analysis of albumin, casein, and the Fn antibody L8 (FnI_9-$FnIII_1$) to fibrillar Fn stretched in a uniaxial strain device. (a) FRET I_A/I_D values in false color for Fn fibers that have incorporated 5% of Fn-DA. (b) Corresponding histogram with calibration lines indicating the I_A/I_D ratios of soluble Fn denatured by GdnHCl in solution. (c) Fluorescence intensity of BSA labeled with Alexa Fluor 633 (BSA-633) adsorbed to Fn fibers. Absolute fiber strains shown were defined as $100(L\text{-}Lo)/Lo$, where L is the extended fiber length and Lo is the fiber length when fully relaxed. (d) The corresponding plot giving the BSA-633 intensity normalized per labeled Fn. The color bar represents the number of pixels with a given I_A/I_D ratio of fibrillar Fn and BSA intensity. The medians are given as white dots. Panels (e−h) and (i−l) show the same data anlysis displayed for casein and Fn antibody L8, respectively. Data averages obtained from 10 fields of views for albumin, casein and for all proteins in whole bovine serum are shown in the Supplements (Figure S4). (Please note that our FRET ratios were not corrected for minute crosstalk between the excitation and emission channels, since absolute distances were not calculated here.)

significantly decreased once they were stretched beyond the onset of FnIII module unfolding (1 M GdnHCL). This phenomenon is likely explained by the disruption of L8's binding site as the relative position between FnI_9 and $FnIII_1$ is mechanically increased.

Enhanced Albumin and Casein Binding Correlates with the Force-Induced Unfolding of FnIII Modules. Since albumin and casein binding significantly increases when the Fn fibers are stretched, we asked how and whether this correlates with the force-induced unfolding of FnIII modules. Since two of the 15 FnIII modules of a Fn monomer each contain a buried cysteine residue that is only exposed upon denaturation or upon forced unfolding (on $FnIII_7$ and $FnIII_{15}$), we used an assay developed by Johnson et al.,[12] where cysteine-labeling dyes were utilized to indicate the force-induced exposure of buried cysteine residues in the intracellular proteins.[31] In a control, iodoacetamide was used to alkylate-exposed hydrophobic patches in different Fn starting formations.[32] Using these two assays, we show that stretching of the Fn fibers exposes the buried cysteines on $FnIII_7$ and $FnIII_{15}$ (Figure 2a−g) and that cysteine exposure increases with mechanical strain (Figure 2h,i), similar to recent data from our group conducted on freely suspended fibers (Klotzsch et al., submitted). To investigate the low strain region, the fibers were deposited (140% strain) on a prestrained silicone sheet that was then fully relaxed (0% strain). Since forces of a few μN are needed to pull the Fn fibers out of a droplet, they are prestrained to approximately 140% strain when they are deposited onto the silicone sheets (Klotzsch et al., submitted). Any possible free cysteines exposed on the now relaxed Fn fibers were blocked with iodoacetamide. Afterward, the fibers were stretched in increments, and the newly exposed cysteines in each increment were allowed to react with maleimide dye from solution. To investigate the high strain region in a second set of experiments, the Fn fibers were now deposited (140% strain) on a relaxed silicone sheet. The free cysteines were first blocked with iodoacetamide. The fibers were then stretched and stained with maleimide dye in increments until a 550% absolute fiber strain was reached. In a control experiment, it could be demonstrated that alkylation of the buried cysteins of Fn in a denaturing solution prior to assembling the fibers and stretching them blocked all maleimide binding sites (Figure 2b−d). These data suggest that the fraction of unfolded FnIII modules increases steadily with mechanical strain.

In contrast to upregulated nonspecific binding of proteins to stretched fibers, stretching reduces the binding of the probe fluorophore bis-ANS (4,4′-dianilino-1,1′-binaphthyl-5,5′-disulfonic acid, dipotassium salt). Bis-ANS has been used to identify structural intermediates in the thermal or chemical unfolding pathways of proteins.[33−39] While bis-ANS in aqueous solution alone has a negligible fluorescence, it turns fluorescent when bound to hydrophobic regions of partially disrupted tertiary structures and decreases again when the secondary structure is destroyed.[39,40] When nonfibrillar Fn is chemically denatured in solution (using GdnHCl), the bis-ANS fluorescence reaches maximal values at about ~0.8 M GdnHCl and then declines upon further denaturation (Supporting Information, Figure S1). Taken together, these findings are in agreement with previous circular dichroism studies, indicating that these are the conditions under which Fn begins to lose secondary structure.[10,27−29] As Fn fibers are stretched, the bis-ANS fluorescence per Fn molecule declines steadily (Figure 2j,k). This trend seen for bis-ANS is in contrast to the increased binding of albumin and casein to stretched fibers (Figure 1), and in agreement with the structural model proposed here.

Stretched Fn Fibers Relax within Minutes Coincident with the Release of Nonspecifically Bound Proteins. Reversibility is a central attribute that has to be met by any protein whose physiological function and functional regulation depends on surviving many stretch and relaxation cycles. It is thus important to ask whether albumin binding to stretched Fn fibers inhibits the structural relaxation of Fn fibers or whether albumin is released from the fiber upon fiber relaxation. In the presence and absence of adsorbed albumin, FRET from fibrillar Fn recovers when the stretched fibers are relaxed, as seen in Figure 3a. While it took about a minute to manually relax the silicone sheet in the strain device and then a few more minutes to refocus, we note that relaxing the Fn fibers can indeed switch their FRET signature. The contraction of the Fn fibers was accompanied by the release of the nonspecifically bound proteins (Figure 3b). Upon restretching, the I_A/I_D ratio changes back to the original value.

Specific Fn−Fn Binding Sites on the Fibrils Are Not Blocked by Nonspecific Protein Binding. To address whether nonspecific binding of albumin might block specific binding sites on Fn fibers, we probed how the exposure of the Fn−Fn binding sites depends on the mechanical strain of the fibers. Fn−Fn binding sites are found on the N-terminal FnI modules and on various FnIII modules,[6,41] and it has been shown previously that cell-generated forces acting on Fn are needed to induce Fn fibrillogenesis either ex vivo[42−44] or in cell culture.[45] Images of Fn fibers at various strains show indeed that soluble Fn binds more strongly to stretched (horizontal orientation) rather than to relaxed (vertical orientation) fibers (Figure 4); full-length soluble Fn as well as its N-terminal 70 kDa fragment (domains $FnI_1-FnIII_1$) show the same stretch upregulated trend. The pixel-by-pixel correlations in Figure 4d show more quantitatively that the binding of soluble Fn-633 normalized by the number of fibrillar Fn molecules increases first gently until the fibers reach 100−140% absolute strain, followed by a steep increase at higher strains (Figure 4d). In contrast, while the Fn's 70 kDa fragment also showed an increase in binding to mechanically stretched Fn fibers (Figure 4e−h), its most significant increase occurred before the fibers were stretched to 100−140% absolute strain (see also Figure S5, Supporting Information). One explanation for the enhanced binding of the 70 kDa fragment at low fiber strain could be that low tensions induce a conformational change within $FnIII_1-FnIII_2$, opening up a cryptic site that upregulates the binding of the 70 kDa fragment,[41,45,46] or in any other mechanosensitive regions. In contrast, binding of full-length

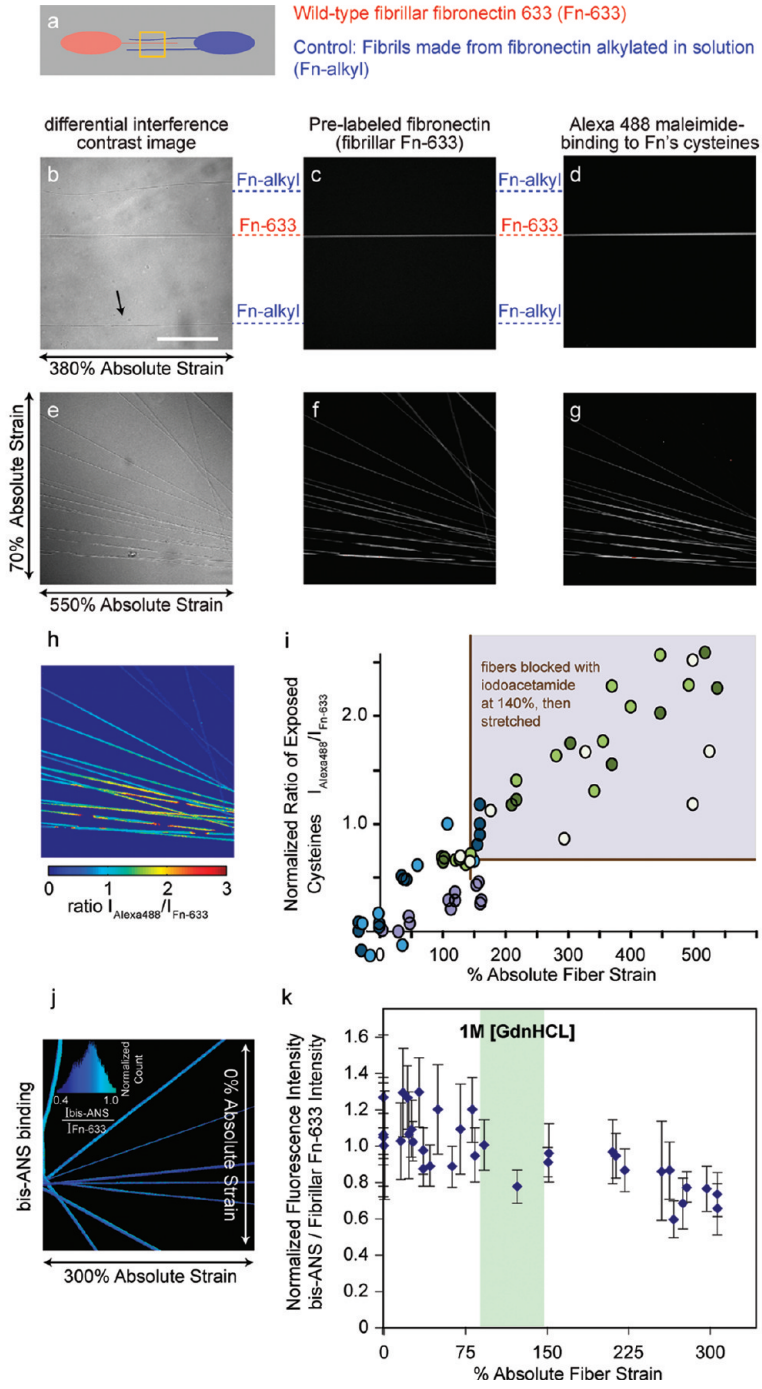

Figure 2. Force-induced exposure of cryptic cysteines on $FnIII_7$ and $FnIII_{15}$ evaluated with iodoacetamide and bis-ANS binding to Fn fibers physisorbed to silicone sheets. (a) Fibers were pulled from a drop of wild-type Fn (blue) and deposited onto a silicone sheet that was mounted into a uniaxial stretch device.[14] As a negative control, a drop of alkylated Fn (red) randomly labeled with Alexa 633 on lysines was positioned at the opposite side, and fibers were pulled and deposited in between fibers of alkylated Fn. (b) Differential interference contrast image of prepared fiber sample after it had been washed and stretched in BPS buffer containing 2% BSA. (c) Fluorescence emission of Alexa 633 conjugated to 5% of the fibrillar Fn molecules. (d) Alexa 488 maleimide binding to stretch-exposed cryptic binding sites. After stretching, 5 ng of Alexa 488 maleimide were added to the solution and allowed to react for 15 min. (e−i) Differentially strained Fn fibers that were deposited under various angles to the strain axis. After deposition, all exposed hydrophobic patches on these fibers were blocked with iodoacetamide. Data analysis was performed by calculating the Alexa 488 to Fn-633 ratios. (j−k) Stretch-dependent binding of bis-ANS to Fn fibers. Fn fibers containing 5% Alexa Fluor 633-labeled Fn (Fn-633) were manually deposited onto prestretched silicon sheets in various orientations and subjected to a 0 and a 300% absolute strain, as indicated. Bis-ANS was then adsorbed for 45 min to the substrates, and the ratio of bis-ANS over the Fn-633 intensity was calculated for each pixel ((j) inset histogram). The intensity ratio was converted into a false shade of blues, where lighter colors indicated a greater degree of bis-ANS binding, and was displayed in the spatially resolved representative image shown. (k) The intensity ratio of the bix-ANS over the Fn-633 fluorescence, computed pixel-by-pixel, for 48 fibers oriented in various directions versus their absolute strain. Scale bar in (b) is 100 μm.

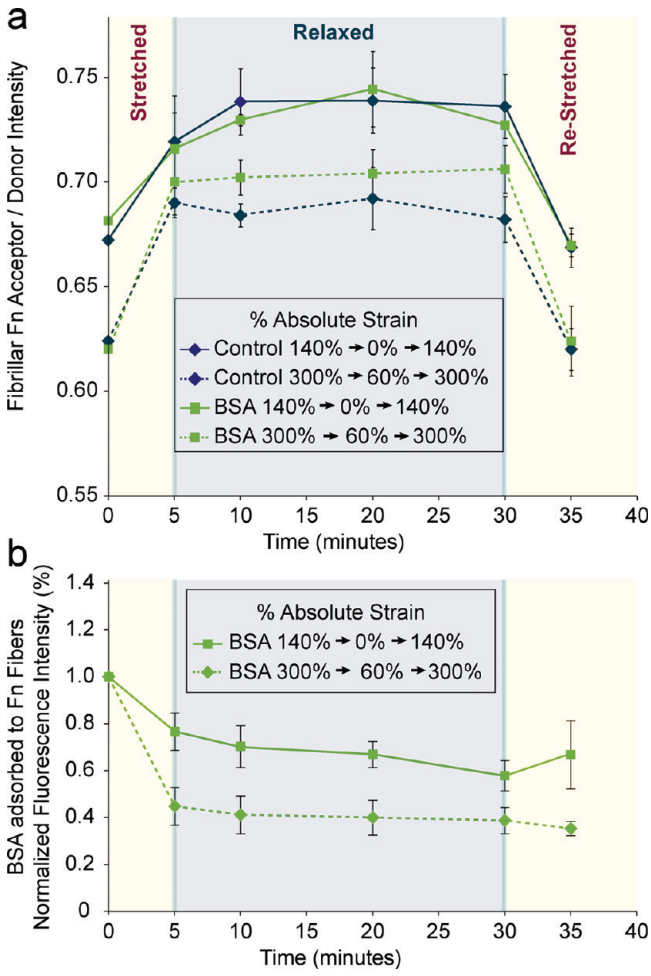

Figure 3. Reversibility of switching the FRET signature when relaxing Fn fibers and the associated release of nonspecifically bound proteins. (a) Fn fibers were manually deposited in parallel orientations onto prestrained silicone substrates and incubated with Alexa 633-labeled BSA or nothing as a control. The substrates were imaged for FRET as well as the relative BSA-633 intensity of the bound proteins before and after the indicated absolute strains factor values (b). After imaging at 5, 10, 20, and 30 min, the samples were restretched to their original conformation and again imaged. Each data point represents (a) the mean ± standard deviation of the average acceptor intensity divided by donor intensity (I_A/I_D) per pixel, or (b) the mean ± standard deviation of the normalized average BSA-633 intensity of all pixels that contained Fn to distinguish between protein binding to the background silicone substrate.

Fn to stretched Fn fibers could be increasingly mediated by not just specific but also nonspecific interactions.

Physiological Implications. Since force-dependent cell signaling pathways regulate various cell functions[13,17,47,49] mechanical forces provide living systems with an additional dimension of functional regulation. While the stretching of proteins might allow cells to alter the structure−function relationship of proteins in very specific manners,[4−7,12,13,48,49] stretch-induced unfolding also comes with a price. As shown here for Fn fibers, protein stretching unravels secondary structure, leading to the exposure of cryptic and hydrophobic residues (Figures 1, 2, 4 and Supporting Information, Figure S1). Coping with the exposure of fouling hydrophobic patches upon stretch, which might lead to adverse downstream consequences in a physiological environment, such as the nonspecific adsorption of other proteins, requires their immediate functional rescue. Here, we show that albumin and casein, if present at physiological concentrations, can serve in this role as they rapidly block newly exposed hydrophobic sites (Figure 1). Our data might thus provide a previously unrecognized physiological explanation for why such high concentrations of these proteins are found in body fluids.

Since cells go through rapid cycles of contraction and spreading,[49] each of which will stretch and release ECM fibers, how fast can ECM fibers recover their fully relaxed length when released? We recently showed that also freely suspended stretched Fn fibers could fully relax and refold within minutes in buffer solution (Klotzsch et al., submitted), but no previous information was available that demonstrated whether stretched Fn fibers could relax in the presence of serum proteins. Here, we show that stretched Fn fibers deposited on silicone sheets have contracted within minutes (Figure 3a). Fiber relaxation appears to be possible through the release of nonspecifically bound proteins, as experimentally demonstrated by labeling albumin with a third color (Figure 3b).

While demonstrated here for ECM fibers, many other force-bearing proteins exist in tissues and include all of the proteins that physically link the cell exterior to the interior.[48] Since force-induced protein unfolding has been demonstrated for intracellular proteins as well (for review, see refs 12, 13, and 48), we would like to propose that intra- and extracellular molecular chaperones might have dual functions. They might not just recognize misfolded or thermally denatured proteins, but one of their key functions could be to rapidly block and thereby pacify stretch-induced hydrophobic residues of extra- and intracellular proteins. In support of this hypothesis, it was shown already that mechanical stress induces the expression of heat shock proteins.[50]

In summary, deciphering the mechanisms by which proteins can be utilized as mechanochemical signal converters is of fundamental importance to many areas of research. While the molecular design principles by which force can activate or eliminate protein binding are slowly emerging for a variety of proteins (as reviewed in ref 48), we illustrate here that molecular chaperones might play an essential role in preventing unwanted hydrophobic−hydrophobic interactions caused by mechanically stretched and unfolded proteins in physiological environments. Thus, molecular chaperones might play an additional and not yet recognized role: our data suggest that they are essential and enabling players in mechanotransduction processes where proteins are employed by cells as molecular switches that convert mechanical into biochemical signals via force-induced unfolding processes. To be effective, mechanical chaperones must have a high relative concentration, a k_{on} fast enough to compete effectively with other proteins, and the k_{off} has to be fast enough to not inhibit refolding once the tension is released.

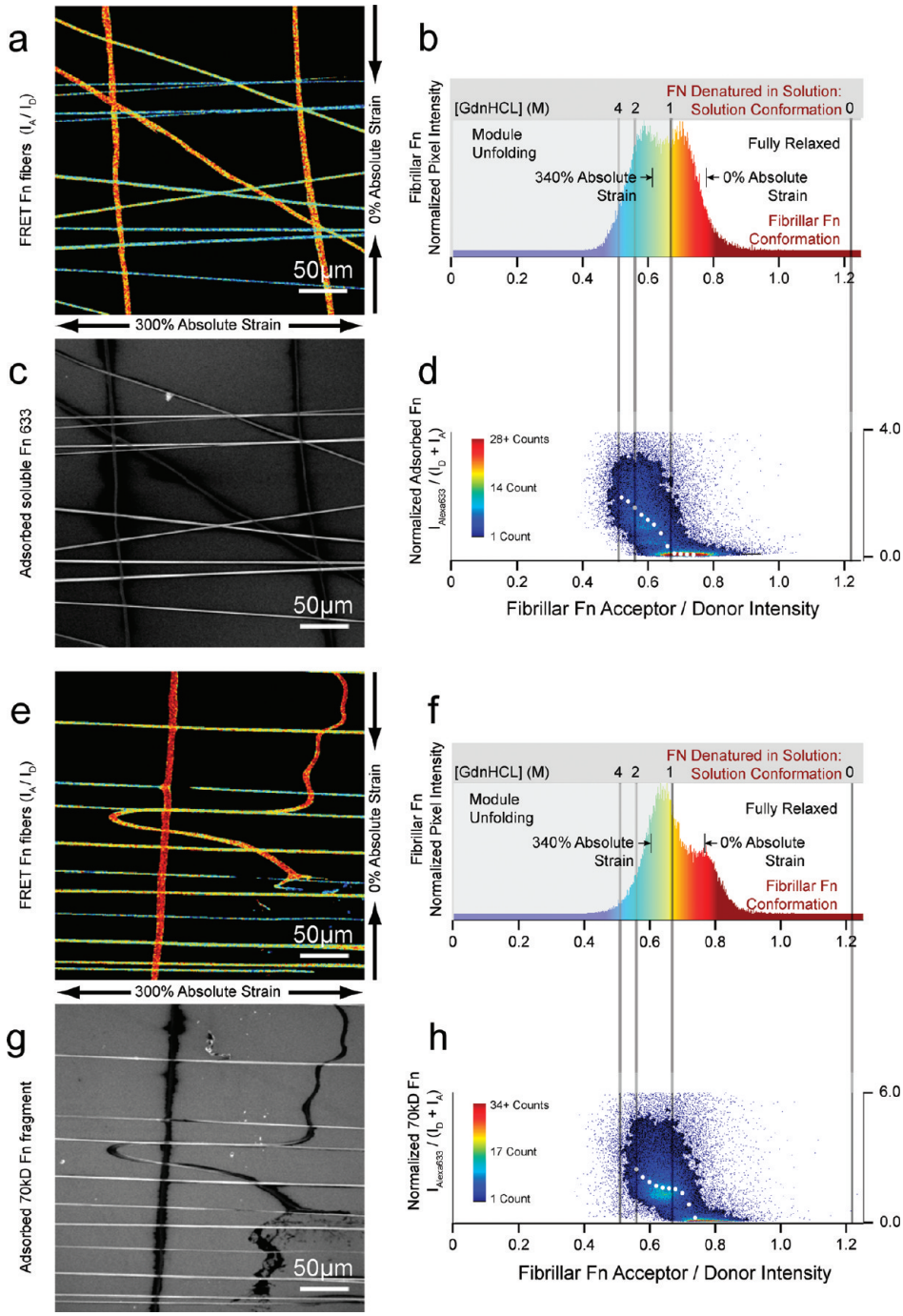

Figure 4. Colocalization analysis of soluble Fn and the 70 kDa Fn fragment binding to stretched or relaxed fibrillar Fn. The data were analyzed and displayed analogous to the ones shown in Figure 1. (a−d) Full-length Fn and (e−h) is its 70 kD N-terminal fragment.

Methods. Isolation and Fluorescent Labeling of Fibronectin. Fn was isolated from human plasma (Swiss Red Cross) via a previously described procedure[10,14,51] and dual-labeled (Fn-DA) with Alexa Fluor 488 succinimidyl ester and Alexa Fluor 546 maleimide for FRET experiments, also as previously described.[14] The eluant solution from the final step of the labeling procedure was determined via spectrophotography to have Fn labeled on average with 6.0 donors (Alexa Fluor 488) and 3.6 acceptors (Alexa Fluor 546). This batch of Fn-DA, which was the only one used to collect data for this report, was stored in frozen 10 μL aliquots and only used when thawed for less than 5 days.

Mechanical Strain and Chemical Unfolding Calibrations, Microscopy, and FRET Analysis. The batch of soluble Fn-DA used in this report was first calibrated for chemically induced unfolding in increasing GdnHCl solutions as described previously.[14] Images were acquired via scanning laser confocal microscopy (Olympus FV-1000), and the degree of intramolecular FRET was probed pixel-by-pixel by dividing the intensity of the acceptor channel by the intensity of the donor channel (I_A/I_D), as previously described.[14] To establish an I_A/I_D versus mechanical strain calibration curve, a 0.3 g/L solution of 95% unlabeled Fn and 5% Fn-DA was used to manually deposit Fn fibers onto

relaxed or prestrained rectangular silicone sheets. The fibers were then rinsed four times and then equilibrated in a phosphate buffered saline (PBS) solution and then subsequently strained or relaxed to defined amounts in a custom-built one-dimensional strain device at room temperature described previously.[14]

Colocalization Analysis of Protein Binding to Fibrillar Fn. In order to quantitatively describe the relationship between the binding of a protein from solution to the conformation of fibrillar Fn, samples of manually deposited Fn fibers were prepared as described above. BSA, casein, and the 70 kDa Fn fragment were acquired from Sigma, and along with the isolated Fn described above, both proteins were labeled with Alexa Fluor 633 fluorophores on random amines following the manufacture's protocol. Each protein was incubated with the samples for 10 min at room temperature (at solution concentrations: BSA and casein, 100 μg/mL; Fn, 3 μg/mL; 70 kD Fn, 1 μg/mL) and rinsed with a PBS or 2% BSA solution before imaging. Because the z-resolution of the confocal microscope was 1 μm, the middle slice of the fibers was taken for all data analysis. For all adsorbed surfaces, we observed that the fiber interior was brightly fluorescent as well, indicating that the interior is accessible to soluble proteins. Experiments were also repeated with widely varying concentrations and incubation times, and the results did not change (data not shown). Furthermore, to block nonspecific adsorption, samples with casein and the 70 kDa Fn fragment were preincubated with a 2% BSA solution for 1 h before introduction of the labeled protein. To block specific adsorption and test for nonspecific adsorption alone, samples of Fn were incubated with a 100× more concentrated solution of unlabeled protein before introduction of the labeled protein. In addition, the mouse antihuman L8 monoclonal antibody, received as a generous gift from Michael Chernousov, was adsorbed at a 1:200 dilution for 10 min to samples blocked for 1 h with a 2% BSA solution before rinsing with 2% BSA and incubating for another 10 min with a 1:200 dilution of a Cy5 donkey antimouse secondary antibody (Jackson Antibody). As a control, incubation with the Cy5 secondary antibody alone was performed, and no background adsorption to the fibers was observed (data not shown).

Fn Refolding and Release of Adsorbed Proteins. To study refolding kinetics of fibrillar Fn and the release of bound proteins, 5% Fn-DA fibers were manually deposited in parallel orientations onto prestrained substrates, rinsed four times with PBS, and incubated with BSA-633 (at 100 μg/mL) or nothing as a control. After imaging the fiber samples in an initial absolute 140 or 300% strain (average I_A/I_D of 0.67 and 0.62, respectively; Figure 3a), the fibers were relaxed to 0 ("fully relaxed") or 60% strain. Then, we imaged again at 5, 10, 20, and 30 min. After this point, the samples were again stretched to their initial conformations and imaged a final time at the same original field of view. In addition to recording the average I_A/I_D values of individual fibers at each time and position point, the intensity of each far-red channel pixel (633 nm excitation, 645−745 nm detection) was normalized by the intensity of the acceptor channel only (546 nm excitation, 566−578 nm detection). Because the intensity of the substrate Fn increased significantly upon fiber relaxation, the donor channel could not be kept constant or used in the normalization analysis without saturating the PMT. The average ratio of the intensity of bound protein to the intensity of the directly excited acceptor for each pixel comprising a fiber was then plotted as in Figure 3b.

Bis-ANS Binding and Analysis. Fn fibers were manually deposited from a 0.3 g/L solution of 10% Alexa Fluor 633-labeled Fn (Fn-633) onto prestrained silicone substrates in a "star"-like pattern and, upon full relaxation of the substrate (0% strain), produced a population of Fn known to have a fully relaxed conformation and another with a strained conformation (300% strain; Supporting Information, Figure S2A). To detect the exposure of hydrophobic patches on the intact secondary protein structure, a 0.4 mM solution of bis-ANS was incubated for 45 min on the fiber samples and rinsed four times with PBS. Experiments were also repeated with 1 h or 10 min incubation times, and the results did not change. Images were acquired by exiting the samples with laser wavelengths of 454 and 633 nm while collecting emitted light between 475−575 nm (Channel 1) and 645−745 nm (Channel 2). Using a custom script written in Ruby (www.ruby-lang.org) together with image analysis software (ImageMagick Software Suite, www.imagemagick.org), the background from each channel was subtracted and a 1 pixel radius Gaussian blur (with a 1 pixel standard deviation) was applied to smooth errant intensity values before the intensity of the bis-ANS channel was divided by the intensity of the corresponding Fn-633 channel. This ratio was then mapped to false shades of blue, as shown in Figure 2j and plotted in the histogram. To determine the strain factor (l) of fibers deposited at an angle (θ) to the stretch axis of substrates relaxed by a factor of ε with a transverse extension factor of ε_T, the following equation was used

$$l = \left(\left(\frac{\cos\theta}{\varepsilon}\right)^2 + \left(\frac{\sin\theta}{\varepsilon_T}\right)^2\right)^{-1/2}$$

Iodocetamide Experiments. To further investigate the exposure of hydrophobic residues, we compared Fn fibers pulled from a labeled Fn solution with fibers pulled out of a solution where the hydrophobic residues were already alkylated in denaturant. Fibers were pulled from a drop of Fn treated with iodoacetamide, which oxidizes free sulphides to prevent maleimide dye binding, in the presence of denaturant. Then, the drop of alkylated Fn was removed. A drop of wild-type human serum Fn labeled with Alexa 633 on lysines was positioned at the opposite side, and fibers were pulled and deposited in between fibers of alkylated Fn. The drop of Alexa 633 Fn was removed. After washing the sample, the substrate was stretched under 4% BSA. Finally, 5 ng of Alexa 488 maleimide was added to the solution and incubated for 15 min to investigate where/if it is able to bind to the newly exposed hydrophobic patches. In a second set of experiments, we investigated 633-labeled Fn fibers deposited on polydimethylsiloxan (PDMS) sheets as before in different starting positions (star shape) but then blocked the already exposed hydrophobic patches on these fibers with iodoacetamide. After we applied

uniaxial stretch to the substrate and therewith stretched or orthogonally relaxed the fibers, we added Alexa 488 maleimide. Data analysis was performed by calculating the Alexa 488 to 633 fluorescence ratios.

Image Analysis. To determine FRET from Fn fibrils, the field of view was excited with 488 nm light, and the respective fluorescence intensities were determined for the donor channel (514−526 nm) and acceptor channel (566−578 nm), pixel-by-pixel, to determine I_A/I_D when excited at 488 nm or 633 nm, respectively. For colocalization analyses, a third image of the same field of view was acquired in the far-red channel (645−745 nm) with 633 nm excitation light to detect the intensity of the adsorbed protein. Since fiber diameters are random and also change dramatically with strain, we next sought to normalize the intensity of the fluorescent, soluble binding receptor with the mass of Fn in each pixel. This normalized colocalization data was acquired using a custom script written with Ruby and Imagemagick to produce contour plots of the normalized protein intensity. Briefly, in addition to the handling of the data to produce the I_A/I_D ratios, histograms, and false color image maps as described previously,[14] the script also background subtracted and applied a 1 pixel radius Gaussian blur (with a 1 pixel standard deviation) to the far-red channel. In order to normalize for stretch-related changes in Fn density, the emission intensity of Alexa 633-BSA to the amount of Fn present in each pixel was divided by the sum of the corresponding donor and acceptor channel intensities ($I_A + I_D$). Although this analysis assumes that the quantum efficiency of detecting emission from the donor and acceptor is equivalent, this analysis was similar to a normalization scheme where $I_{Alexa633}$ was divided by the intensity of the acceptor fluorophore but with direct 543 nm excitation. With direct excitation of Alexa 546, energy transfer as well as crosstalk from Alexa 488 into the Alexa 546 emission window was minimal. However, in order to reduce the number of images acquired with each sample, the sum of $I_A + I_D$ was used for all analysis in the present study. From the same field of view as the raw protein−633 channel (Figure 1c), the donor and acceptor channels were acquired, and the standard spatially resolved FRET analysis was performed to produce I_A/I_D histograms (Figure 1b), as described previously.[10,14] Overlaid on the contour plot in Figure 1d between the area corresponding to the fully relaxed and fiber breakage zone conformations is the median normalized intensity for the corresponding I_A/I_D bin from the contour plot of the same data as shown in Figure 1h.

Acknowledgment. The authors gratefully acknowledge Kristopher Kubow and John Saeger for their helpful discussions and Sheila Luna Morris for her help in preparing the figures. This work was financially supported by the ETH Zurich, the Human Frontier Science Program Organization (M.L.S.), the Volkswagen Stiftung, the Nanomedicine Development Center (NDC) "Nanotechnology Center for Mechanics in Regenerative Medicine" (NIH Grant PN2 EY016586), which is part of the NIH Nanomedicine Development Center Network (NNDCN), and an Advanced Investigator Award for Interdisciplinary Research from the European Research Council (V.V.). The mouse antihuman L8 monoclonal antibody was a generous gift from Dr. Michael Chemousov. The authors declare no competing financial interests.

Supporting Information Available: Additional figures. This material is available free of charge via the Internet at http://pubs.acs.org.

Abbreviations

ECM, extracellular matrix
Fn, fibronectin
FRET, fluorescence resonance energy transfer
Fn-DA, Fn labeled with donor and acceptor fluorophores
GdnHCL, guanidine hydrochloride
I_A/I_D, ratio of the acceptor intensity divided by the donor intensity
bis-ANS, 4,4′-dianilino-1,1′-binaphthyl- 5,5′-disulfonic acid, dipotassium salt
L8, monoclonal Fn antibody (epitope: residues 526−675 spanning FnI_9 and $FnIII_1$)
BSA, bovine serum albumin
PBS, phosphate buffered saline

References

(1) Kellermayer, M. S.; Smith, S. B.; Granzier, H. L.; Bustamante, C. Folding−unfolding transitions in single titin molecules characterized with laser tweezers. *Science* **1997**, *276*, 1112–1116.
(2) Rief, M.; Gautel, M.; Oesterhelt, F.; Fernandez, J. M.; Gaub, H. E. Reversible unfolding of individual titin immunoglobulin domains by AFM. *Science* **1997**, *276*, 1109–1112.
(3) Tskhovrebova, L.; Trinick, J. Titin: properties and family relationships. *Nat. Rev. Mol. Cell Biol.* **2003**, *4*, 679–689.
(4) Bustamante, C.; Chemla, Y. R.; Forde, N. R.; Izhaky, D. Mechanical processes in biochemistry. *Annu. Rev. Biochem.* **2004**, *73*, 705–748.
(5) Muller, D. J.; et al. Single-molecule studies of membrane proteins. *Curr. Opin. Struct. Biol.* **2006**, *16*, 489–495.
(6) Vogel, V. Mechanotransduction involving multimodular proteins: converting force into biochemical signals. *Annu. Rev. Biophys. Biomol. Struct.* **2006**, *35*, 459–488.
(7) Sotomayor, M.; Schulten, K. Single-molecule experiments in vitro and in silico. *Science* **2007**, *316*, 1144–1148.
(8) Fernandez, J. M.; Li, H. Force-clamp spectroscopy monitors the folding trajectory of a single protein. *Science* **2004**, *303*, 1674–1678.
(9) Baneyx, G.; Baugh, L.; Vogel, V. Coexisting conformations of fibronectin in cell culture imaged using fluorescence resonance energy transfer. *Proc. Natl. Acad. Sci. U.S.A.* **2001**, *98*, 14464–14468.
(10) Smith, M. L.; et al. Force-Induced Unfolding of Fibronectin in the Extracellular Matrix of Living Cells. *PLoS Biol.* **2007**, *5*, e268.
(11) Baneyx, G.; Baugh, L.; Vogel, V. Fibronectin extension and unfolding within cell matrix fibrils controlled by cytoskeletal tension. *Proc. Natl. Acad. Sci. U.S.A.* **2002**, *99*, 5139–5143.
(12) Johnson, C. P.; Tang, H. Y.; Carag, C.; Speicher, D. W.; Discher, D. E. Forced unfolding of proteins within cells. *Science* **2007**, *317*, 663–666.
(13) Sawada, Y.; et al. Force sensing by mechanical extension of the Src family kinase substrate p130Cas. *Cell* **2006**, *127*, 1015–1026.
(14) Little, W. C.; Smith, M. L.; Ebneter, U.; Vogel, V. Assay to mechanically tune and optically probe fibrillar fibronectin conformations from fully relaxed to breakage. *Matrix Biol.* **2008**, *27*, 451–461.
(15) Hytonen, V. P.; Vogel, V. How force might activate talin's vinculin binding sites: SMD reveals a structural mechanism. *PLoS Comput. Biol.* **2008**, *4*, e24.
(16) Krammer, A.; Craig, D.; Thomas, W. E.; Schulten, K.; Vogel, V. A structural model for force regulated integrin binding to fibronectin's RGD-synergy site. *Matrix Biol.* **2002**, *21*, 139–147.
(17) Balaban, N. Q.; et al. Force and focal adhesion assembly: a close relationship studied using elastic micropatterned substrates. *Nat. Cell Biol.* **2001**, *3*, 466–472.
(18) Munevar, S.; Wang, Y.; Dembo, M. Traction force microscopy of migrating normal and H-ras transformed 3T3 fibroblasts. *Biophys. J.* **2001**, *80*, 1744–1757.

(19) Tan, J. L.; et al. Cells lying on a bed of microneedles: an approach to isolate mechanical force. *Proc. Natl. Acad. Sci. U.S.A.* **2003**, *100*, 1484–1489.
(20) Wang, N.; Ostuni, E.; Whitesides, G. M.; Ingber, D. E. Micropatterning tractional forces in living cells. *Cell Motil. Cytoskeleton* **2002**, *52*, 97–106.
(21) Hoffman, A. S. Non-fouling surface technologies. *J. Biomater. Sci., Polym. Ed.* **1999**, *10*, 1011–1014.
(22) Marini, I.; Moschini, R.; Corso, A. D.; Mura, U. Chaperone-like features of bovine serum albumin: a comparison with alpha-crystallin. *Cell Mol. Life Sci.* **2005**, *62* (24), 3092–3099.
(23) Quinlan, G. J.; Martin, G. S.; Evans, T. W. Albumin: biochemical properties and therapeutic potential. *Hepatology* **2005**, *41*, 1211–1219.
(24) Fasano, M.; et al. The extraordinary ligand binding properties of human serum albumin. *IUBMB Life* **2005**, *57*, 787–796.
(25) Fiat, A. M.; Jolles, P. Caseins of various origins and biologically active casein peptides and oligosaccharides: structural and physiological aspects. *Mol. Cell. Biochem.* **1989**, *87*, 5–30.
(26) Morgan, P. E.; Treweek, T. M.; Lindner, R. A.; Price, W. E.; Carver, J. A. Casein proteins as molecular chaperones. *J. Agric. Food Chem.* **2005**, *53* (7), 2670–2683.
(27) Yousefi, R.; Shchutskaya, Y. Y.; Zimmy, J.; Gaudin, J. C.; Moosavi-Movahedi, A. A.; Muronetz, V. I.; Zuev, Y. F.; Chobert, J. M.; Haertle, T. Chaperone-like activities of different molecular forms of beta-casein. Importance of polarity of N-terminal hydrophilic domain. *Biopolymers* **2009**, *91* (8), 623–632.
(28) Baugh, L.; Vogel, V. Structural changes of fibronectin adsorbed to model surfaces probed by fluorescence resonance energy transfer. *J. Biomed. Mater. Res.* **2004**, *69A*, 525–534.
(29) Khan, M. Y.; Medow, M. S.; Newman, S. A. Unfolding transitions of fibronectin and its domains. Stabilization and structural alteration of the N-terminal domain by heparin. *Biochem. J.* **1990**, *270*, 33–38.
(30) Chernousov, M. A.; Faerman, A. I.; Frid, M. G.; Printseva, O.; Koteliansky, V. E. Monoclonal antibody to fibronectin which inhibits extracellular matrix assembly. *FEBS Lett.* **1987**, *217*, 124–128.
(31) Tsai, R.; Rodriguez, P.; Discher, D. E. Cys shotgun labeling of macrophages adhering to and engulfing Ig-opsonized cells. *Transfus. Clin. Biol.* **2008**, *15*, 58–61.
(32) McKeown-Longo, P. J.; Mosher, D. F. Mechanism of formation of disulfide-bonded multimers of plasma fibronectin in cell layers of cultured human fibroblasts. *J. Biol. Chem.* **1984**, *259*, 12210–12215.
(33) Kumar, R.; Peerschke, E. I.; Ghebrehiwet, B. Zinc induces exposure of hydrophobic sites in the C-terminal domain of gC1q-R/p33. *Mol. Immunol.* **2002**, *39*, 69–75.
(34) Hong, D. P.; Hagihara, Y.; Kato, H.; Goto, Y. Flexible loop of beta 2-glycoprotein I domain V specifically interacts with hydrophobic ligands. *Biochemistry* **2001**, *40*, 8092–8100.
(35) Panda, M.; Smoot, A. L.; Horowitz, P. M. The 4,4′-dipyridyl disulfide-induced formation of GroEL monomers is cooperative and leads to increased hydrophobic exposure. *Biochemistry* **2001**, *40*, 10402–10410.
(36) Egelund, R.; et al. A regulatory hydrophobic area in the flexible joint region of plasminogen activator inhibitor-1, defined with fluorescent activity-neutralizing ligands. Ligand-induced serpin polymerization. *J. Biol. Chem.* **2001**, *276*, 13077–13086.
(37) Bethell, R. C.; Gray, N. M.; Penn, C. R. The kinetics of the acid-induced conformational change of influenza virus haemagglutinin can be followed using 1,1′-bis(4-anilino-5-naphthalenesulphonic acid). *Biochem. Biophys. Res. Commun.* **1995**, *206*, 355–361.
(38) Goto, Y.; Fink, A. L. Conformational states of beta-lactamase: molten-globule states at acidic and alkaline pH with high salt. *Biochemistry* **1989**, *28*, 945–952.
(39) Semisotnov, G. V.; et al. Study of the "molten globule" intermediate state in protein folding by a hydrophobic fluorescent probe. *Biopolymers* **1991**, *31*, 119–128.
(40) Horowitz, P. M.; Butler, M. Interactive intermediates are formed during the urea unfolding of rhodanese. *J. Biol. Chem.* **1993**, *268*, 2500–2504.
(41) Karuri, N. W.; Lin, Z.; Rye, H. S.; Schwarzbauer, J. E. Probing the conformation of the fibronectin III1−2 domain by fluorescence resonance energy transfer. *J. Biol. Chem.* **2008**, *284*, 3445−3452.
(42) Ulmer, J.; Geiger, B.; Spatz, J. P. Force-induced fibronectin fibrillogenesis in vitro. *Soft Matter* **2008**, *4*, 1998–2007.
(43) Baneyx, G.; Vogel, V. Self-assembly of fibronectin into fibrillar networks underneath dipalmitoyl phosphatidylcholine monolayers: role of lipid matrix and tensile forces. *Proc. Natl. Acad. Sci. U.S.A.* **1999**, *96*, 12518–12523.
(44) Wojciak-Stothard, B.; Denyer, M.; Mishra, M.; Brown, R. A. Adhesion, orientation, and movement of cells cultured on ultrathin fibronectin fibers. *In Vitro Cell Dev. Biol.: Anim.* **1997**, *33*, 110–117.
(45) Zhong, C.; et al. Rho-mediated contractility exposes a cryptic site in fibronectin and induces fibronectin matrix assembly. *J. Cell Biol.* **1998**, *141*, 539–551.
(46) Vakonakis, I.; Staunton, D.; Rooney, L. M.; Campbell, I. D. Interdomain association in fibronectin: insight into cryptic sites and fibrillogenesis. *Embo J.* **2007**, *26*, 2575−2583.
(47) Discher, D. E.; Janmey, P.; Wang, Y. L. Tissue cells feel and respond to the stiffness of their substrate. *Science* **2005**, *310*, 1139–1143.
(48) Vogel, V.; Sheetz, M. P. Cell fate regulation by coupling mechanical cycles to biochemical signaling pathways. *Curr. Opin. Cell. Biol.* **2009**, *21*, 38–46.
(49) Vogel, V.; Sheetz, M. Local force and geometry sensing regulate cell functions. *Nat. Rev. Mol. Cell Biol.* **2006**, *7* (4), 265–275.
(50) Chano, T.; Tanaka, M.; Hukuda, S.; Saeki, Y. Mechanical stress induces the expression of high molecular mass heat shock protein in human chondrocytic cell line CS-OKB. *Osteoarthritis Cartilage* **2000**, *8*, 115–119.
(51) Engvall, E.; Ruoslahti, E. Binding of soluble form of fibroblast surface protein, fibronectin, to collagen. *Int. J. Cancer* **1977**, *20*, 1–5.

NL902365Z